

Chalcogenide-based optical parametric oscillator at 2 μm

NURMEMET ABDUKERIM,* LIZHU LI, AND MARTIN ROCHETTE

Department of Electrical and Computer Engineering, 3480 University Street, McGill University, Montréal H3A 0E9, Canada

*Corresponding author: nurmemet.abudukelimu@mail.mcgill.ca

Received 28 June 2016; revised 25 August 2016; accepted 26 August 2016; posted 26 August 2016 (Doc. ID 269188); published 14 September 2016

We report the first chalcogenide-based optical parametric oscillator (OPO) relying on pure parametric gain. The all-fiber OPO operates in the wavelength range of 2 μm and is tunable over 290 nm from the combined Stokes and anti-Stokes contributions. The gain medium is a 10 cm long chalcogenide microwire made from a high modal confinement As_2Se_3 core with cyclo olefin polymer cladding, leading to optimized chromatic dispersion, high nonlinearity, and broadband transparency. With a power threshold of only a fraction of a milliwatt, this design is promising for the fabrication of tunable, compact, and low-power consumption mid-infrared sources. © 2016 Optical Society of America

OCIS codes: (190.4410) Nonlinear optics, parametric processes; (190.4370) Nonlinear optics, fibers; (190.4970) Parametric oscillators and amplifiers.

<http://dx.doi.org/10.1364/OL.41.004364>

Optical parametric oscillators are the most efficient and flexible sources to access broadband or unconventional wavelength bands [1]. Confined within an optical fiber path, fiber optical parametric oscillators (FOPOs) provide the additional advantages of compactness, mechanical stability, reliability of operation, beam quality, and easy integration with fiber systems [2]. A number of FOPO designs have been proposed that, together, cover the transparency range of silica glass. While wavelengths at 2 μm and above are important for chemical sensing applications, FOPOs designed for these wavelengths are limited by the relatively large attenuation and low nonlinearity of silica. In 2010, Gershikov *et al.* demonstrated the operation of a FOPO at a wavelength of 2 μm . The FOPO was enabled by a 200 m long highly nonlinear silica fiber, leading to propagation losses of 15 dB and a required 30 W of pump power to reach the oscillation threshold [3].

As an alternative to silica, chalcogenide glasses (e.g., As_2Se_3 , As_2S_3) are intrinsically highly nonlinear and transmit mid-infrared light at wavelengths up to 12 μm [4]. A most interesting approach is to use microwire geometry, providing the flexibility of the chromatic dispersion parameters and an enhancement of the nonlinear effects [5–9]. By an appropriate

design of the chromatic dispersion properties, chalcogenide microwires can yield significant parametric gain spanning over a broad spectral range [10].

Ahmad *et al.* reported the first Raman-assisted FOPO based on chalcogenide glass, using an As_2Se_3 microwire to generate parametric oscillation at output wavelengths of 1.605 (Stokes) and 1.502 μm (A-Stokes) [11]. However, wavelength tunability was limited to the Raman gain bandwidth of only a few nanometers.

In this Letter, we demonstrate the first chalcogenide-based FOPO that oscillates from pure parametric gain. The broad oscillation spectrum of the FOPO is divided into two sections: a first set of wavelengths for which the gain originates from a pure parametric process, and a second set of wavelengths for which the gain is a combination of parametric and Raman processes. The FOPO is tunable from 1.980 to 2.142 μm (Stokes) and from 1.770 to 1.898 μm (A-Stokes). The average power threshold of the FOPO is 487 μW with a slope efficiency of 2%. This demonstration is an important step toward the development of compact and tunable, compact and low-power consumption optical sources for the mid-infrared.

The microwire used in this investigation is fabricated from a three-layer composite that consists of an inner core of As_2Se_3 , an intermediate layer of cyclo olefin polymer (COP), and an outer layer of poly-methyl methacrylate (PMMA) [12]. Figure 1 presents a schematic of the microwire composition and geometry. The microwire has a uniform diameter profile results from the careful tapering of a section of hybrid fiber [13]. In this structure, the large refractive index contrast between As_2Se_3 core ($n_{\text{As}_2\text{Se}_3} = 2.81$) and COP cladding ($n_{\text{COP}} = 1.48$) tightly confines the optical mode in the microwire core and enables chromatic dispersion engineering. The COP cladding preserves transparency in the 2 μm wavelength band and ensures optical insulation of the evanescent wave from the ambient environment.

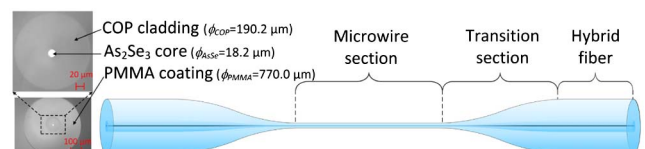


Fig. 1. Hybrid microwire composition and geometry (not to scale) with the reflection optical micrograph of its facet.

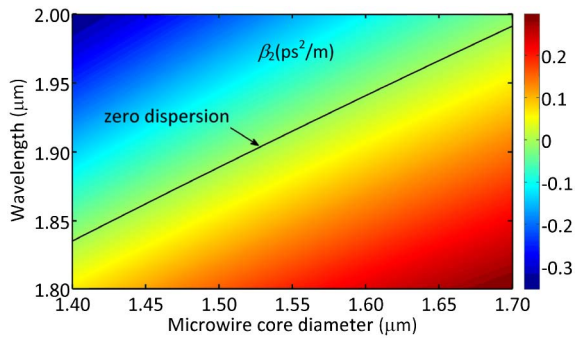


Fig. 2. Group velocity dispersion β_2 (in ps^2/m) for the fundamental mode of the microwire as a function of the core diameter. The zero dispersion wavelength with corresponding microwire core diameter is illustrated by the solid line.

The group velocity dispersion β_2 of the fundamental mode propagating in the microwire can be engineered to zero, normal, or anomalous, depending on the target application [14]. Figure 2 shows the group velocity dispersion spectrum of the fundamental mode as a function of the microwire core diameter.

Parametric gain is present when the pump and signal wavelengths satisfy the phase-matching condition of degenerate four-wave mixing [15]. Figure 3(a) shows second- and fourth-order dispersion coefficients (β_2 and β_4) of the hybrid

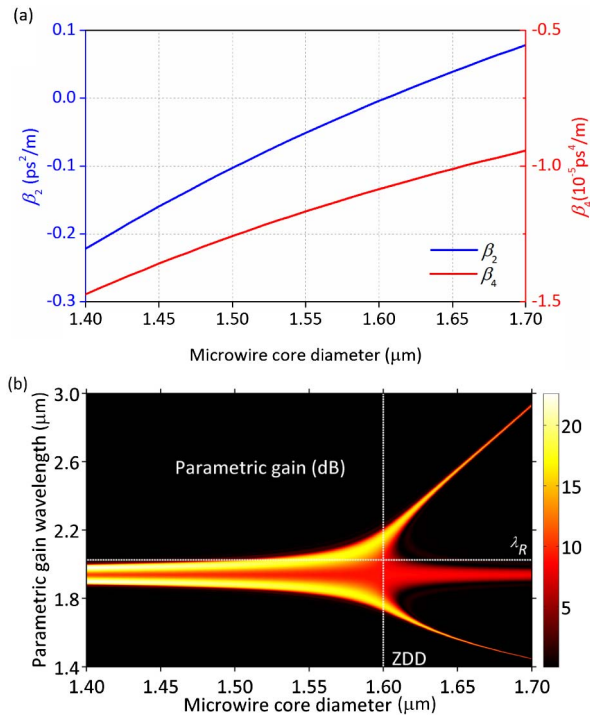


Fig. 3. Simulations for the hybrid As_2Se_3 -COP microwire. (a) Second- and fourth-order dispersion coefficients of the fundamental mode as a function of the microwire core diameter at a wavelength of $1.938 \mu\text{m}$. (b) Parametric gain spectrum (in dB) of a 10 cm long microwire as a function of the core diameter. The peak pump power is 2.4 W at a wavelength of $1.938 \mu\text{m}$. The dashed lines indicate the positions of a zero dispersion diameter (ZDD) and maximum Raman gain wavelength (λ_R).

As_2Se_3 -COP microwire as a function of the core diameter at a wavelength of $1.938 \mu\text{m}$. The sixth- and higher-order dispersion coefficients are neglected, given the relatively small frequency shift of interest. Figure 3(b) shows the parametric gain expected in a 10 cm long microwire with a peak pump power of 2.4 W , using a propagation matrix method [16]. The wavelength at which the Raman gain maximum occurs ($2.025 \mu\text{m}$) is indicated by a horizontal dashed line [17]. A microwire with a core diameter of $\sim 1.55 \mu\text{m}$ has a Raman gain maximum that superimposes at the same wavelength as the parametric gain maximum. A narrow band parametric gain is achieved at a core diameter in excess of $1.6 \mu\text{m}$, where β_2 is positive and β_4 is negative [18].

The microwire used in this investigation is designed with a core diameter of $1.47 \mu\text{m}$, combined with a high optical confinement and a high nonlinear refractive index of As_2Se_3 ($n_2 = 7.6 \times 10^{-18} \text{ m}^2/\text{W}$ at $1.94 \mu\text{m}$ [19]), leading to a high waveguide nonlinearity of $\gamma = 24 \text{ W}^{-1} \text{ m}^{-1}$ and a zero dispersion wavelength of $\lambda_{\text{ZD}} = 1.875 \mu\text{m}$. The lengths of the microwire and transition sections are 10 and 2 cm, respectively. Both ends of the hybrid fiber are polished and butt-coupled to SMF-28 via UV-cured epoxy and result in a SMF-to-SMF insertion loss of 8 dB, including a 0.3 dB/cm of propagation loss at $2 \mu\text{m}$ in the microwire due to COP absorption and diameter nonuniformities and 0.5 dB per interface due to the Fresnel reflection loss at the chalcogenide-silica interfaces; the rest is attributed to mode-mismatch and misalignment losses.

Two sets of experiments are described next: the first set of experiments focuses on the single-pass parametric gain of a hybrid As_2Se_3 -COP microwire, whereas the second set of experiments employs this gain medium to make an optical parametric oscillator. In the first set of experiments, the single-pass parametric gain is measured with a pump-probe configuration. Pump pulses with a full-width at half-maximum (FWHM) duration of 800 fs are provided by a 30 MHz thulium-doped mode-locked fiber laser with a central wavelength of $1.938 \mu\text{m}$. The pulses are amplified by a thulium-doped fiber amplifier and, subsequently, filtered by a 2 nm FWHM tunable bandpass filter to lengthen the pulse duration to $\sim 3 \text{ ps}$ FWHM, as well as to eliminate the amplified spontaneous emission noise from the fiber amplifier. A wavelength-tunable thulium fiber laser is constructed following [20] and serves as a continuous wave probe signal. The probe signal linewidth is $< 0.05 \text{ nm}$, limited by optical spectrum analyzer resolution bandwidth. The pump and probe are coupled into the microwire via an 80/20 silica fiber coupler. The polarization states of the pump and probe are co-aligned using polarization controllers. The parametric gain of the probe is measured as a function of the probe wavelength from 1.955 to $2.040 \mu\text{m}$. The average pump power coupled into the microwire is 0.23 mW corresponds to a peak power of 2.4 W , while the input probe power is kept at 0.025 mW . Figure 4(a) shows the output spectra recorded on an optical spectrum analyzer with a dynamic range $> 55 \text{ dB}$, and a resolution bandwidth set to 1 nm and a sampling interval set to 0.1 nm . The amplified signals and generated idlers are pulsed as a consequence of the pulsed pump. Parametric signal gain and idler conversion gain values for each probe signal wavelength are extracted by integrating amplified signal sidebands and idler spectra, and calculating the ratio between the amplified signal/idler peak power and probe signal average

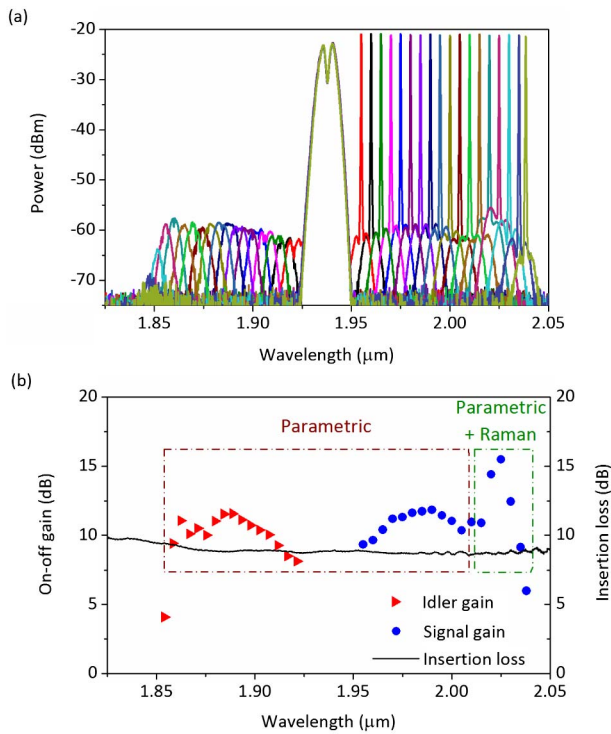


Fig. 4. (a) Superimposition of single-pass parametric amplification spectra resulting from several probe wavelengths. (b) On-off parametric signal gain (blue circles), idler conversion gain (red triangles), and insertion loss of the pigtailed microwire (black solid line).

power [21]. Figure 4(b) shows the signal and idler gain as a function of the wavelength. The microwire provides an optical gain resulting from the superimposition of a broad parametric gain and Raman gain. A maximum gain of 15.5 dB occurs at a wavelength of 2.025 μm , corresponding to the Raman frequency shift in As_2Se_3 , that is $\Delta f \sim 6.7$ THz or $\Delta\lambda \sim 87$ nm with respect to the pump wavelength. The measured parametric gain is lower than the theoretical value by up to 9 dB as a result of random diameter fluctuations and, thus, longitudinal dispersion fluctuation along the length of the microwire [22,23].

Figure 5 presents the FOPO as a result of inserting the gain medium in a resonant cavity. The FOPO is composed of a wavelength-selective coupler to combine the pump pulses in

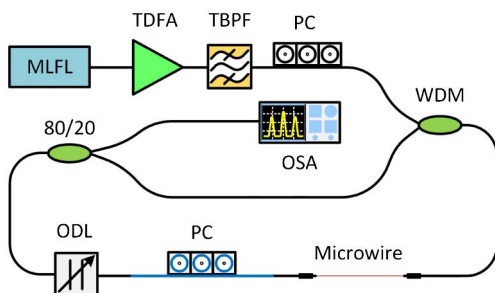


Fig. 5. Experimental setup of the FOPO. MLFL, mode-locked fiber laser; TDFA, thulium-doped fiber amplifier; TBPF, tunable bandpass filter; WDM, wavelength division multiplexing coupler; PC, polarization controller; ODL, optical delay line; OSA, optical spectrum analyzer.

the cavity and extract them after one round-trip, a tunable optical delay line (ODL) to precisely adjust the cavity length according to the repetition rate of the pump laser, a polarization controller (PC) to ensure that the oscillating pulses always get back to their initial polarization state when entering the microwire, and an 80/20 broadband fiber coupler to sample the in-cavity power. The PC is composed of a 3.4 m long high numerical aperture and normal dispersion fiber to partially compensate for the total cavity dispersion. All the components with the exception of the microwire and the PC are made with SMF-28 fiber, which has an anomalous dispersion at 2 μm . Total cavity dispersion is slightly anomalous with ~ 0.09 ps/nm at 2.023 μm . At the output coupler, 80% of the signal is fed back to the cavity, and 20% serves to monitor the signal.

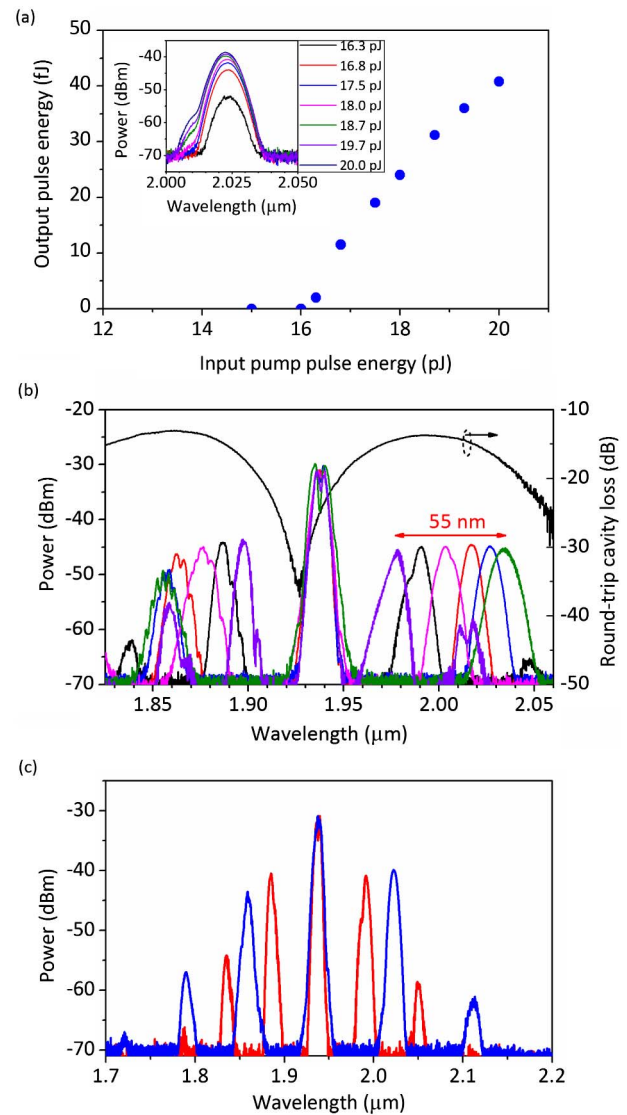


Fig. 6. (a) Output signal pulse energy versus the input pump pulse energy. Inset: output signal spectrum evolution with an increasing input pump pulse energy. (b) Output spectra of the FOPO for various delay settings. The black curve shows the FOPO round-trip cavity loss. (c) Output spectra of the FOPO showing first- and second-order parametric oscillation. The delay line is adjusted for first-order Stokes set at 2.023 μm (blue) and 1.991 μm (red).

The FOPO reaches the oscillation threshold when the total nonlinear gain exceeds the total round-trip loss of 14 dB, and when the cavity length enables the synchronization of the pump and oscillating pulses. Figure 6(a) shows the output signal pulse energy as a function of the input pump pulse energy for the FOPO output at a wavelength of 2.023 μm . The threshold pump pulse energy is 16.2 pJ, corresponding to 5 W of peak power, with a slope efficiency of 2%. The inset shows the evolution of the FOPO output signal optical spectrum as the input pump pulse energy increases. A slight tendency for saturation in the output pulse energy is observed due to pump depletion. At higher pump power levels, undesired nonlinear effects (e.g., self-phase modulation, cross-phase modulation, supercontinuum generation) appear because of high nonlinearity in the microwire. These undesired nonlinear effects can be avoided by increasing the pump pulse width or by shortening the microwire.

The FOPO is wavelength-tuned by adjusting the cavity length via the optical delay line with a rate of ~ 10 nm/ps. Figure 6(b) shows the spectra of the FOPO at several wavelengths. On the long wavelength side (Stokes), the FOPO wavelength is continuously tuned from 1.980 to 2.035 μm , corresponding to a total tuning range of 55 nm. This wavelength span exceeds the Raman gain bandwidth and, thus, the FOPO oscillation is maintained solely by a parametric gain in the wavelength range of 1.980 to ~ 2.005 μm . The input pump pulse energy requires up to 25.5 pJ to access the complete tuning range. On the short wavelength side (A-Stokes), the FOPO wavelength is continuously tuned from 1.850 to 1.898 μm , corresponding to a total tuning range of 48 nm. The shortest walk-off length between the pump pulses and the oscillating signal pulses in the microwire is ~ 18 cm. This is almost twice as long as the microwire and, thus, temporal walk-off is not expected to play an important role on the performance of the FOPO.

The FOPO also shows evidence of cascaded parametric oscillation, as noticed from Fig. 6(b). Figure 6(c) shows two FOPO outputs for two positions of the optical delay line. The first orders of the FOPO can be tuned from 1.980 to 2.035 μm (Stokes) and 1.850 to 1.898 μm (A-Stokes), whereas the second orders can be tuned from 2.024 to 2.142 μm (Stokes) and 1.770 to 1.859 μm (A-Stokes). Thus, in total, the FOPO is tunable over a spectral range of 290 nm.

In conclusion, we have demonstrated the first 2 μm band FOPO using a highly nonlinear chalcogenide microwire. The parametric gain of the FOPO is sufficiently strong to support oscillation without the support of Raman gain. The FOPO has a low peak pump power threshold of 5 W and a slope efficiency of 2%. The first-order oscillating signal can be tuned from 1.980 to 2.035 μm on the Stokes side and from 1.850 to 1.898 μm on the A-Stokes side. With the help of

cascaded four-wave mixing, the FOPO can cover a total tunable wavelength range of 290 nm. The FOPO has a lower threshold and a higher slope efficiency, compared to previously reported FOPOs in the same wavelength band [3,24].

Funding. Collaborative Research and Development Grants Program of the Natural Sciences and Engineering Research Council of Canada (NSERC).

Acknowledgment. The authors are grateful to Coractive High-Tech for providing the chalcogenide glass used in the experiments.

REFERENCES

1. M. H. Dunn and M. Ebrahimzadeh, *Science* **286**, 1513 (1999).
2. M. E. Marhic, *Fiber Optical Parametric Amplifiers, Oscillators and Related Devices* (Cambridge University, 2008).
3. A. Gershikov, E. Shumakher, A. Willinger, and G. Eisenstein, *Opt. Lett.* **35**, 3198 (2010).
4. J. S. Sanghera, I. D. Aggarwal, L. B. Shaw, C. M. Florea, P. Pureza, V. Q. Nguyen, and F. Kung, *J. Optoelectron. Adv. Mater.* **8**, 2148 (2006).
5. P. Dumais, A. Villeneuve, P. G. J. Wigley, F. Gonthier, S. Lacroix, G. I. Stegeman, and J. Bures, *Opt. Lett.* **18**, 1996 (1993).
6. M. A. Foster, A. C. Turner, M. Lipson, and A. L. Gaeta, *Opt. Express* **16**, 1300 (2008).
7. E. C. Mägi, L. B. Fu, H. C. Nguyen, M. R. E. Lamont, D. I. Yeom, and B. J. Eggleton, *Opt. Express* **15**, 10324 (2007).
8. C. Baker and M. Rochette, *Opt. Express* **18**, 12391 (2010).
9. C. Baker and M. Rochette, *IEEE Photon. J.* **4**, 960 (2012).
10. R. Ahmad and M. Rochette, *Opt. Express* **20**, 9572 (2012).
11. R. Ahmad and M. Rochette, *Opt. Express* **20**, 10095 (2012).
12. L. Li, A. Al-kadry, N. Abdukerim, and M. Rochette, *Opt. Mater. Express* **6**, 912 (2016).
13. C. Baker and M. Rochette, *Opt. Mater. Express* **1**, 1065 (2011).
14. J. A. Buck, *Fundamentals of Optical Fibers* (Wiley, 2004).
15. G. P. Agrawal, *Nonlinear Fiber Optics* (Academic, 2007).
16. M. Farahmand and M. de Sterke, *Opt. Express* **12**, 136 (2004).
17. R. E. Slusher, G. Lenz, J. Hodelin, J. Sanghera, L. B. Shaw, and I. D. Aggarwal, *J. Opt. Soc. Am. B* **21**, 1146 (2004).
18. T. Godin, Y. Combes, R. Ahmad, M. Rochette, T. Sylvestre, and J. M. Dudley, *Opt. Lett.* **39**, 1885 (2014).
19. G. Lenz, J. Zimmermann, T. Katsufuji, M. E. Lines, H. Y. Hwang, J. S. Sanghera, and I. D. Aggarwal, *Opt. Lett.* **25**, 254 (2000).
20. G. Xue, B. Zhang, K. Yin, W. Yang, and J. Hou, *Opt. Express* **22**, 25976 (2014).
21. X. P. Liu, R. M. Osgood, Y. A. Vlasov, and W. M. J. Green, *Nat. Photonics* **4**, 557 (2010).
22. D. Chow, J. C. Nouni, A. Denisov, J. C. Beugnot, T. Sylvestre, L. Li, R. Ahmad, M. Rochette, K. H. Tow, M. A. Soto, and L. Thévenaz, in *Frontiers in Optics* (Optical Society of America, 2015), paper FW4F-4.
23. M. Karlsson, *J. Opt. Soc. Am. B* **15**, 2269 (1998).
24. B. Kuyken, X. P. Liu, R. M. Osgood, R. Baets, G. Roelkens, and W. M. J. Green, *Opt. Express* **21**, 5931 (2013).